The Effect of Particle Collisions on Heat Transfer in a Non-Isothermal Dilute Turbulent Gas-Particle Flow

Hamid Reza Zandi Pour[1], Michele Iovieno[1]
[1]Dipartimento di Ingegneria Meccanica e Aerospaziale, Politecnico di Torino
Corso Duca degli Abruzzi 24, 10129 Torino, Italy
hamid.zandipour@polito.it; michele.iovieno@polito.it

Abstract – We analyze the effect of particle-to-particle collision on the heat transfer in a temporally evolving thermal mixing layer which develops between two isothermal regions in a homogeneous and isotropic turbulent flow. Eulerian-Lagrangian Direct Numerical Simulations in the two-way coupling regime are carried out in a wide range of particle Stokes number, from 0.2 to 3, with a thermal Stokes-number-to-Stokes-number ratio equal to 4.43, at a Taylor microscale Reynolds number up to 124. We quantify how much particle collisions tend to reduce the average heat transfer with respect to a collisionless regime and show that the overall effect is minor even at the higher Stokes number simulated.

Keywords: heat transfer, particle-laden flow, turbulent mixing, inter-particle collisions

1. Introduction

Particle-laden turbulent flows are ubiquitous, as they can be found in a wide range of applications such as, for example, liquid fuel combustion, warm rain formation, dispersion of pollutants in atmosphere, and the coexistence of plankton species and plastic particle agglomeration in oceans, which have kept it an active area of research in many scientific disciplines for decades. Although this complex problem has been being experimentally investigated in the context of turbulence, direct numerical simulations(DNSs) have been always an important tool to obtain detailed results on features which cannot be directly measured, primarily due to the difficulties in Lagrangian measurements. Moreover, they allow to focus on some physical aspects only of the complex problem. However, DNSs are limited to relatively low to medium Reynolds numbers due to the need for huge computational resources. Particle-fluid thermal interaction has been studied in many papers, mainly within the point–particle approach valid for small sub-Kolmogorov particles, mainly in channel flows [1–3] and in homogeneous turbulence [4–6]. In a few recent works we have studied the fluid-particle thermal interaction in time-evolving shearless thermal mixing layer which is generated by the interaction between two fluid regions with different temperatures. This basic configuration is also apt to be used as benchmark for turbulence models. Both one-way and two-way coupling regimes have been considered [7, 8] in a collisionless suspension. The effect of particle inertia and Reynolds number have been discussed.

Collisions between particles have important effect on the heat transfer in fluidized beds, because heavy particles cross the wall layer bringing heat to/from the wall to the core region of the pipe. However, in these applications volume fractions are much higher, of the order of 10^{-2}, and beyond the limit of two-way coupling between point particles [9]. There are only just a few theoretical work which consider collisions, as [10] who analytically studies the heat transferred between particles during an elastic collision. Normally, the effect of collisions is not taken into account when dealing with heat transfer by particles, even if inter-particle collisions become more frequent as the volume fraction increases. The effect of particle-particle collision on temperature statistics has been studied by Carbone et al. [5] in homogeneous and isotropic turbulence in the one-way coupling regime, finding a minor effect on small-scale temperature statistics. However, collisions have the dynamical effect to decelerate small particles while accelerating large particles, thus producing an enhanced velocity scattering. In presence

of a strong temperature gradient, that may affect their ability to carry enthalpy over long distances, which is the phenomenon through which particles enhance the heat transfer with respect to an unseeded flow [8] .

Therefore, to investigate the effect of inter-particle collisions on the heat transfer and on fluid-particle correlations, we extend our previous works, by considering the effect of collisions on the heat transfer in the simplest inhomogeneous flow configuration, where heat is transferred between two regions at different temperatures by a statistically homogeneous and isotropic velocity field. The imposed initial temperature difference correlates temperature and velocities in the mixing layer which develops at the boundary between the two isothermal regions. The results are compared with the collisionless regime in the same overall flow configuration [8].

The content of the paper is as follows. The physical model and numerical methods employed to simulate the collisional turbulent gas-solid flow are described in section 2 in detail. Results from direct numerical simulations are discussed in section 3. This includes a comparison between the Nusselt number variation in terms of Stokes number and Taylor micro-scale Reynolds number for collisional and collisionless flow regimes. Main conclusions are briefly summarized in section 4.

2. Methodology

2.1. Governing equations

We present the mathematical model of the dynamics of a non isothermal incompressible flow seeded with particles in an Eulerian-Lagrangian approach, where the continuous fluid phase is distinguished by the discrete particle phase. Temperature variations are assumed to be small enough not to produce relevant density changes so that the fluid temperature can be represented as an advected passive scalar. Therefore, the fluid phase is described by the following system,

$$\frac{\partial u_i}{\partial x_i} = 0, \tag{1}$$

$$\frac{\partial u_i}{\partial t} + u_j \frac{\partial u_i}{\partial x_j} = -\frac{1}{\rho_0} \frac{\partial p}{\partial x_i} + \nu \frac{\partial^2 u_i}{\partial x_j \partial x_j} + f_{u,i}, \tag{2}$$

$$\frac{\partial T}{\partial t} + u_j \frac{\partial T}{\partial x_j} = \kappa \frac{\partial^2 T}{\partial x_j \partial x_j} + \frac{1}{\rho_0 c_{p0}} C_T. \tag{3}$$

Here $u(x,t)$, $T(x,t)$, and $p(x,t)$ are fluid velocity, temperature and pressure fields, while ρ_0, c_{p0}, ν, and κ stand for the (constant) fluid density, isobaric specific heat capacity, kinematic viscosity and thermal diffusivity. Moreover, f_u is a body force introduced to keep turbulent fluctuations in a statistically steady state, and C_T is the heat exchanged per unit time and unit mass with particles, i.e. particle thermal back reaction on the flow. Similar to previous works (e.g. [5, 6, 8]), we do not consider the force exerted by particles on the fluid: only fluid temperature field is two-way coupled with particles, and momentum exchange occurs only under one-way coupling regime. This assumption yields in a dilute regime and in our problem because it has been found that momentum feedback has a minor thermal effect on fluid temperature statistics [5].

Particles are assumed to be spheres of radius R much smaller than the Kolmogorov length-scale, so that they can be regarded as material points, and to have a mass density much higher than the fluid density, so that only Stokes drag force is retained in the Maxey–Riley equation for the motion of small particles in a fluid [11]. An analogous equation for the particle temperature can be written under the same hypothesis, so that the dynamics of each particle is governed by the following equations

$$\frac{\mathrm{d}^2 x_{p,i}}{\mathrm{d}t^2} = \frac{\mathrm{d}v_{p,i}}{\mathrm{d}t} = \frac{u_i(t, x_{p,i}) - v_{p,i}}{\tau_v}, \tag{4}$$

$$\frac{\mathrm{d}\vartheta_p}{\mathrm{d}t} = \frac{T(t, x_{p,i}) - \vartheta_p}{\tau_\vartheta}, \tag{5}$$

where $x_p(t)$, $v_p(t)$, and $\vartheta_p(t)$ are position, velocity and temperature of the p-th particle, respectively. Here τ_v and τ_ϑ are the

Table 1: Dimensionless flow parameters.

Simulation		I	II	III
Taylor microscale Reynolds number	Re_λ	56	86	124
Taylor microscale	λ	0.226	0.29	0.35
Integral length scale	ℓ	0.40	0.74	0.94
Root mean square of velocity fluctuations	u'	0.59	0.71	0.85
Forced wavenumber	k_f	5	$\sqrt{6}$	$\sqrt{3}$
Prandtl number	Pr	0.71	0.71	0.71
mean turbulent kinetic energy dissipation rate	ε	0.25	0.25	0.25
Kolmogorov length scale	η	0.0153	0.0153	0.0153
Kolmogorov time scale	τ_η	0.098	0.098	0.098
Particle volume fraction	φ		4×10^{-4}	
Density ratio	ρ_p/ρ_0		10^3	
Stokes number ratio	$\mathrm{St}_\vartheta/\mathrm{St}$		4.43	
Stokes number	St		0.2 ; 0.3 ; 0.5 ; 0.7 ; 0.8 ; 0.9 ; 1 ; 1.2 ; 1.5 ; 2 ; 2.5 ; 3	

momentum and thermal relaxation times, given by

$$\tau_v = \frac{2}{9}\frac{\rho_p}{\rho_0}\frac{R^2}{\nu}, \qquad \tau_\vartheta = \frac{1}{3}\frac{\rho_p c_{pp}}{\rho_0 c_{p0}}\frac{R^2}{\kappa}, \tag{6}$$

where ρ_p, and c_{pp} denote particle density and specific heat at constant pressure. Any direct particle-particle interaction, except collisions, is excluded. Therefore, the particle thermal feedback per unit time and unit volume is given by

$$C_T(x_i, t) = \frac{4}{3}\pi R^3 \rho_p c_{pp} \sum_{p=1}^{N_p} \frac{\mathrm{d}\vartheta_p(t)}{\mathrm{d}t}\delta(x_i - x_{p,i}). \tag{7}$$

2.2. Flow configuration and numerical method

We consider the heat transfer between two homogeneous regions with different temperatures T_1 and $T_2 < T_1$ in a homogeneous and isotropic velocity field. Therefore, we solve the governing equations of sec.2.1 in a parallelepiped domain with sizes $L_1 = L_2$ and $L_3 = 2L_1$ in directions x_1, x_2 and x_3. The initial temperature is set equal to T_1 in the $x_3 < L_3/2$ half-domain and equal to T_2 in the $x_3 > L_3/2$ half-domain. Periodic boundary conditions on all faces are used for velocity, while temperature is decomposed in a mean linear field and a fluctuating part as in [8], so that periodic boundary conditions can be applied to the latter part. Particles which exit the domain reenter at the opposite side.

The equations are made dimensionless by using the shorter size of the domain L_1 over 2π as a length scale, a velocity scale derived from the imposed kinetic energy dissipation ε, and the temperature difference $T_1 - T_2$ as a temperature scale [8]. Results will be presented by using the Taylor-microscale as reference length, which is more dynamically significant. Therefore, in dimensionless form, the flow is governed by the Reynolds number $\mathrm{Re} = u'\lambda/\nu$, the Prandtl number $\mathrm{Pr} = \nu/\kappa$ and by the particle-to-fluid heat capacity ratio $\varphi_\vartheta = \varphi(\rho_p c_{pp})/(\rho_0 c_{p0})$, where φ is the particle volume fraction. Particle dynamics is governed by the ratio between their relaxation times and the flow timescales, which define the Stokes numbers. Since particles respond to local fluctuations of fluid state, the Kolmogorov timescale $\tau_\eta = (\nu/\varepsilon)^{1/2}$ is normally used instead of the large-scale time used in the adimensionalization, so that their dynamics can be described in terms of the Stokes number $\mathrm{St} = \tau_v/\tau_\eta$ and the thermal Stokes number $\mathrm{St}_\vartheta = \tau_\vartheta/\tau_\eta$. All the flow parameters are indicated in table 1.

A fully dealiased (3/2-rule) pseudospectral method is used for the spatial discretization of the fluid phase equations (1–3).

In the Fourier space the forcing $\boldsymbol{f}$ has the following form

$$\hat{f}_{u,i}(t,\boldsymbol{\kappa}) = \varepsilon \frac{\hat{u}_i(t,\boldsymbol{\kappa})}{\sum_{||\boldsymbol{\kappa}||=\kappa_f} ||\hat{u}_i(t,\boldsymbol{\kappa})||^2} \delta(||\boldsymbol{\kappa}|| - \kappa_f), \tag{8}$$

where ε is the imposed energy dissipation and κ_f is the forced wavenumber. A recent new numerical method [12, 13], based on inverse and forward non-uniform fast Fourier transforms with a fourth-order B-spline basis, has been used to interpolate fluid velocity and temperature at particle positions and to compute particle feedback. Both carrier flow (1–3) and particles 4–5) equations are integrated in time by means of a second order exponential integrator.

2.3. Inter-particle collision model

In this work we consider only elastic binary collisions, which occur when the distance between the centres of two particles is equal to their diameter. Elastic collisions are introduced in the numerical simulation after each time step by means of a first order particle trajectory reconstruction. This yields to the following equation for the collision between the p-th and q-th particle in a time step, $t \in [t_n, t_{n+1})$,

$$||(1 - \tilde{t})(\boldsymbol{x}_p(t_n) - (\boldsymbol{x}_q(t_n)) + \tilde{t}(\boldsymbol{x}_p(t_{n+1}) - (\boldsymbol{x}_q(t_{n+1}))|| = 2r_p, \tag{9}$$

where $\tilde{t} = (t - t_n)/\Delta t$. A collision occurs when a real solution of (9) exists for $\tilde{t} \in [0, 1)$. In such a case, the positions and velocities of the colliding particles at the end of the time step are assumed that ones obtained from momentum and energy conservation, i.e. they move with the velocity achieved after the collision for the remaining part of the time step. It is assumed that no heat transfer occurs between colliding particle at impact event and no direct hydrodynamic interaction except inter-particle collisions, is taken into account [14]. From a computational standpoint, direct collision detection is highly time-consuming and is not affordable for a large number of particle N_p, because order $O(N_p^2)$ numerical operations would be needed. Thus, grouping the particles within small boxes and looking for particle inside each box [14] is employed, which is a more practical and computationally affordable approach. In this method, the effect of the box boundaries can be removed by shifting the boxes and repeating the algorithm.

3. Results

We present a comparison between the heat transfer in presence of particles in the collisional and collisionless regimes. All simulations have been carried out within the thermal two-way coupling regime and the thermal Stokes number to Stokes number ratio has been kept constant and equal to 4,43. A visualization of the particles and their temperature is shown in figure 1: particles, advected by the flow, move across the plane initially separating the two regions at different temperatures, being heated or cooled in the process. This flow configuration produces a self-similar stage of evolution, where all the flow and particles statistics collapse when rescaled with the mixing layer thickness δ, which can be defined as $(T_1 - T_2)/\max\{|\partial T/\partial x_3|\}$ [7, 8] and shows an almost diffusive time growth. This stage is achieved after a few eddy turnover times $\tau = \ell/u'$, during which a high temperature variance region develops in the thermally inhomogeneous region. In this stage of evolution, the particle to fluid temperature variance ratio remains constant. One can observe that collisions tend to slightly reduce the variance of particle temperature with respect to the fluid one, as shown in figure 2, especially at larger Stokes numbers.

Figure 3 shows the most important result, that is the correlation between velocity and temperature fluctuations, which are proportional to the mean heat transfer between the two regions at a different temperature. Indeed, the mean heat transfer in the inhomogenenous direction x_3 is given by

$$\dot{q} = -\lambda \frac{\partial \langle T \rangle}{\partial x_3} + \rho_0 c_{p0} \langle u_3' T' \rangle + \varphi \rho_p c_{pp} \langle v_3' \vartheta' \rangle \tag{10}$$

where the first term is the diffusive heat transfer, the second one is the carrier flow convection, and the last one is the particle contribution. By using standard dimensional analysis, it can be written in terms of the Nusselt number, defined as the heat flux
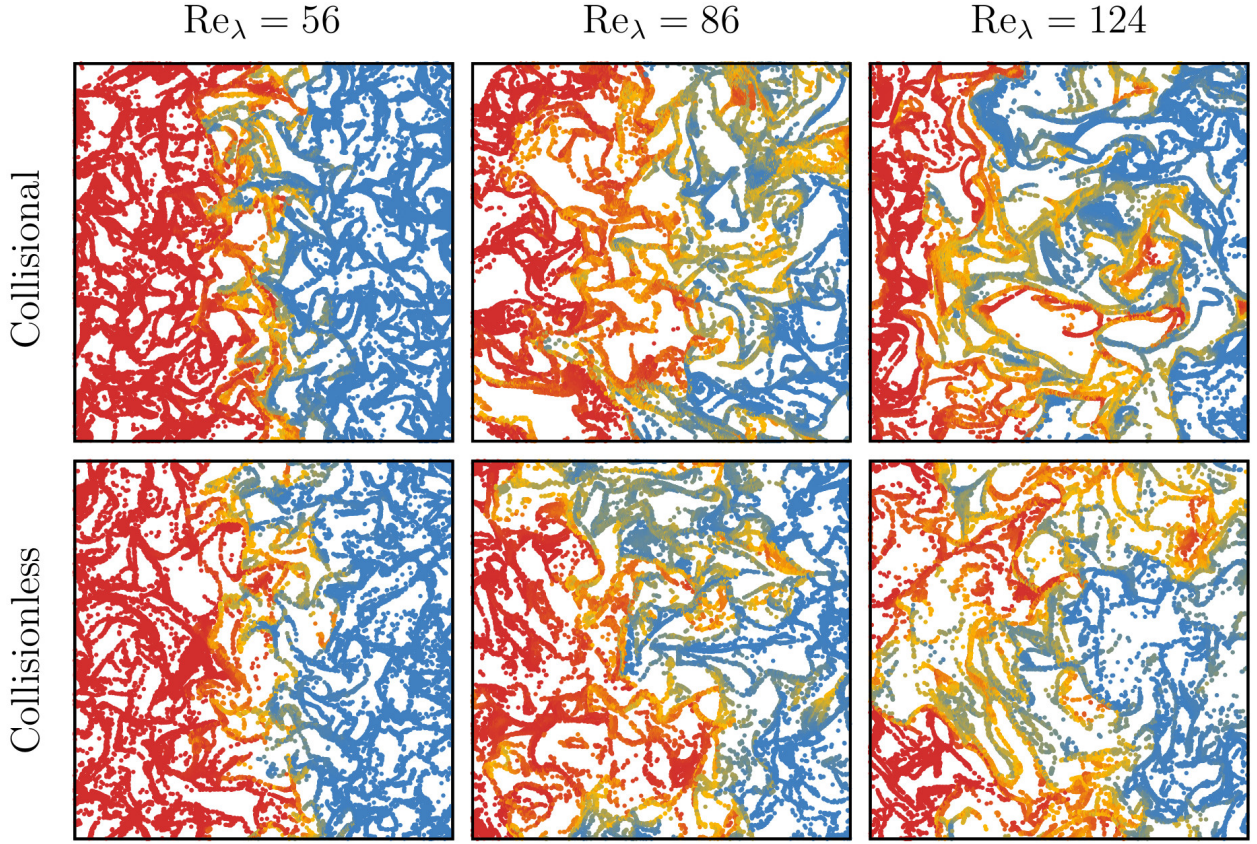
Figure 1: Visualization of particles at $t/\tau = 3$, $\tau = \ell/u'$ in a small slab around a (x_1, x_3) plane. Particles, out of scale, are colored according to their temperature, the red colour corresponds to the maximum temperature in the domain, and the blue colour to the lowest temperature. The upper row shows particles in the collisional regime, while the lower row shows particles in the collisionless regime.

normalized by the heat transfer in a static, non-moving system. In this flow, the mixing layer thickness δ is the only relevant length-scale, so that Nu = $\dot{q}/[\lambda(T_1 - T_2)/\delta]$. Dimensional analysis gives

$$\mathrm{Nu} = \mathrm{Nu}(\mathrm{Re}_\lambda, \mathrm{Pr}, \varphi_\vartheta, \mathrm{St}, \mathrm{St}_\vartheta)$$

where Re_λ is the Reynolds number, Pr is the fluid Prandtl number, $\varphi_\vartheta = \varphi(\rho_p c_{pp})/(\rho_0 c_{p0})$ is the particle-to-fluid heat capacity ratio, St and St_ϑ are the Stokes and thermal Stokes numbers, i.e. the rations between the particle momentum and thermal relaxation times and the Kolmogorov microscale, St = τ_v/τ_η, $\mathrm{St}_\vartheta = \tau_\vartheta/\tau_\eta$. The Stokes and thermal Stokes numbers quantify particle inertia in dimensionless form. From (10), Nu can be decomposed in the flow and particle convection, i.e. Nu = $1 + \mathrm{Nu}_c + \mathrm{Nu}_p$, where

$$\mathrm{Nu}_c = \frac{-\langle u_3' T' \rangle}{\kappa |\partial \langle T \rangle / \partial x_3|}, \qquad \mathrm{Nu}_p = \varphi_\vartheta \frac{-\langle v_3' \vartheta' \rangle}{\kappa |\partial \langle T \rangle / \partial x_3|} \tag{11}$$

The ratio $\mathrm{Nu}_p/\mathrm{Nu}_c$, equal to $\varphi_\vartheta \langle v_3' \vartheta' \rangle / \langle u_3' T' \rangle$, is the parameter which gives a measure of the enhancement of the heat transfer due to the presence of suspended particles. The existence of a self-similar stage implies that the Nusselt number does not depend on time, because all fluxes have the same spatio-temporal evolution, by scaling with the same length $\delta(t)$.
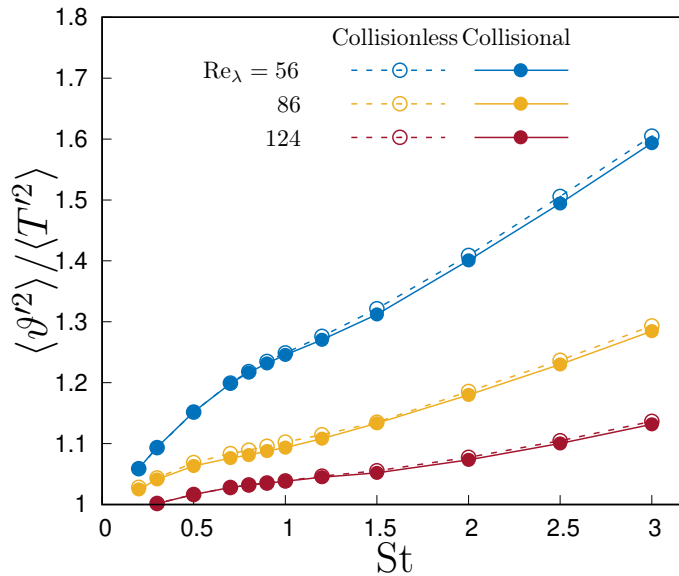
Figure 2: Particle temperature variance to fluid temperature variance ratio in two-way coupling simulations with and without collisions. Variances are measure in the central part of the domain, where heat transfer takes place.
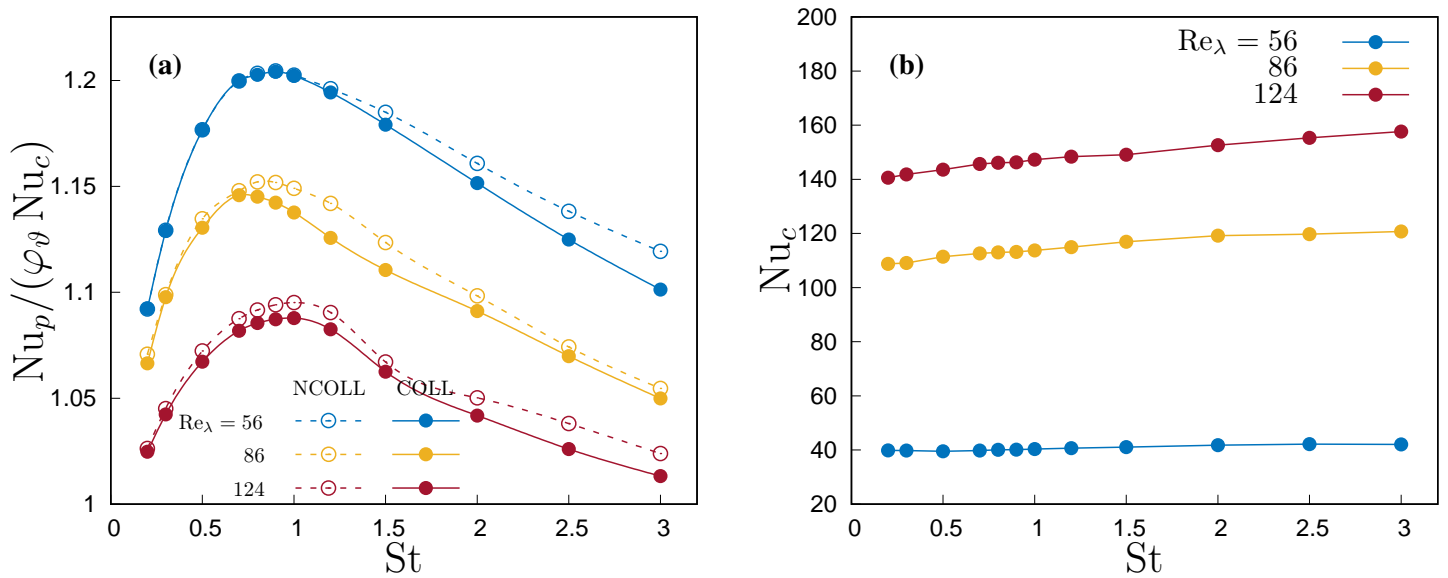

Figure 3: (a) Particle contribution to the Nusselt number as a function of the Stokes number at different Taylor microscale Reynolds numbers. (b) Convective Nusselt number as a function of the Stokes number. Continuous lines indicate the collisional regime, while dashed lines indicate collisionless simulations.
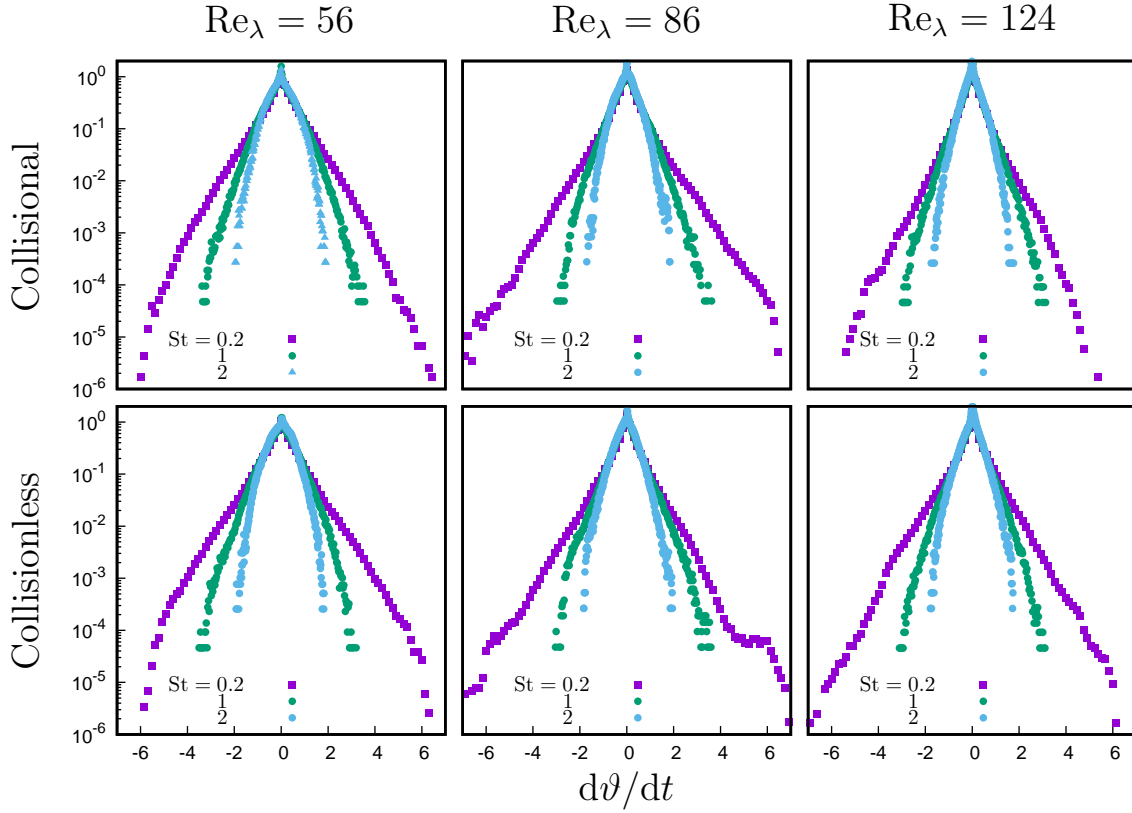
Figure 4: Probability density function of the particle temperature derivative at $t/\tau = 3$ in collisional and collisionless simulations for different Taylor microscale Reynolds number Re_λ for three different Stokes numbers.

Figure 3(a) shows this ratio for three different Reynolds numbers as a function of the Stokes number. All quantities are computed in the centre of the domain. The ratio has a maximum when the Stokes number is of order one, that is, in correspondence of the highest particle clustering. When the Stokes number approaches zero, particles behave like tracers. However, since in our configuration also the thermal Stokes number tends to vanish, they behave like passive tracers, so that $\mathrm{Nu}_p/(\varphi_\vartheta \mathrm{Nu}_c) \to 1$ when $\mathrm{St} \to 0^+$. On the other side, when $\mathrm{St} \to \infty$, particles velocity and temperature tend to decorrelate from the fluid temperature. The same trend can be observed in all the simulated configurations. Figure 3(b) presents the flow convective Nusselt number Nu_c, which shows the effect of temperature modulation by particles.

Collisions between particles have a negligible effect on the convection. This means that, at the volume fraction investigated, the deviation of particles from their trajectory has a minor impact on their feedback on the fluid. However, collisions tend to reduce the particle velocity-temperature correlations and, therefore, the ability of particles to bring heat over long distance. Since collisions between larger particles are likely more common, as expected, the impact on the Nusselt number is more evident as St increase, and become appreciable when $\mathrm{St} > 1$, even if there is always a small reduction, which no more than around 10% even at the highest simulated Stokes number. We could attribute this effect to the fact that collisions between particles with very different temperatures occur between particles coming from the two isothermal region and the scatter due to the collision modifies their velocity in the x_3 direction, thus reducing the $\langle v'\vartheta' \rangle$ correlation.

Figure 4 shows the probability density function of particle temperature time derivative in the central part of the domain at the same dimensionless time. Collisions just have some influence in the tail of the distributions, and have a minor effect when compared with particle thermal feedback on the flow [8], which modulates the carrier flow temperature reducing the fluid–particle temperature difference.

4. Conclusion

In this paper we have analyzed the role of particle collisions on the heat transfer in a thermally coupled particle-laden turbulent flow at a fixed volume fraction $\varphi = 4 \times 10^{-4}$, in the dilute regime where the point-particle approach is valid. We have found that the overall effect is small and negligible when St < 1, while for St > 1 we observed a small reduction of the particle-velocity-temperature correlation, of the order of 10%. Anyway, the effect of collisions on the ability of particles to modulate fluid fluctuations remains almost unchanged. Therefore, we infer that there is no need to introduce collisions in bulk models of heat transfer in particle-laden flows in dilute regimes.

References

[1] F. Zonta, C. Marchioli, and A. Soldati, "Direct numerical simulation of turbulent heat transfer modulation in micro-dispersed channel flow," *Acta Mechanica*, vol. 195, pp. 305–326, 2008.

[2] J. G. M. Kuerten, C. W. M. van der Geld, and B. J. Geurts, "Turbulence modification and heat transfer enhancement by inertial particles in turbulent channel flow," *Phys. Fluids*, vol. 23, no. 12, pp. 123301/1–8, 2011.

[3] F. Rousta and B. Lessani, "Near-wall heat transfer of solid particles in particle-laden turbulent flows," *International Communications in Heat and Mass Transfer*, vol. 112, pp. 104475/1–7, 2020.

[4] J. Béc, H. Homann, and G. Krstulovic, "Clustering, fronts, and heat transfer in turbulent suspensions of heavy particles," *Physical Review Letters*, vol. 112, pp. 234503/1–5, 2014.

[5] M. Carbone, A. D. Bragg, and M. Iovieno, "Multiscale fluid–particle thermal interaction in isotropic turbulence," *J. Fluid Mech.*, vol. 881, pp. 679–721, 2019.

[6] I. Saito, T. Watanabe, and T. Gotoh, "Modulation of fluid temperature fluctuations by particles in turbulence," *J. Fluid Mech.*, vol. 931, p. A6, 2022.

[7] H. R. Zandi Pour and M. Iovieno, "Particle-fluid thermal interaction in free mixing layers," *J. Physics: Conf. Series*, (proceedings of the 39th UIT Heat Transfer International Conference, Gaeta, Italy, 20-22 June 2022, in press).

[8] H. R. Zandi Pour and M. Iovieno, "Heat transfer in a non-isothermal collisionless turbulent particle-laden flow," *Fluids*, vol. 7, no. 11, pp. 345/1–24, 2022.

[9] F. Jiang, H. Wang, Y. Liu, G. Qi, A. E. Al-Rawni, P. Nkomazana, and X. Li, "Effect of particle collision behavior on heat transfer performance in a down-flow circulating fluidized bed evaporator," *Powder Technology*, vol. 381, pp. 55–67, 2021.

[10] J. Sun and M. M. Chen, "A theoretical analysis of heat transfer due to particle impact," *Int. J. Heat Mass Transfer*, vol. 31, pp. 969–975, 1988.

[11] M. R. Maxey and J. J. Riley, "Equation of motion for a small rigid sphere in a nonuniform flow," *Phys. Fluids*, vol. 26, no. 4, pp. 883–889, 1983.

[12] M. Carbone and M. Iovieno, "Application of the non-uniform fast fourier transform to the direct numerical simulation of two-way coupled turbulent flows," *WIT Trans. Eng. Sci.*, vol. 120, pp. 237–248, 2018.

[13] M. Carbone and M. Iovieno, "Accurate direct numerical simulation of two-way coupled particle-laden flows through the nonuniform fast fourier transform," *Int. J. Safety and Sec. Eng.*, vol. 10, no. 2, pp. 191–200, 2020.

[14] R. Onishi, K. Takahashi, and J. C. Vassilicos, "An efficient parallel simulation of interacting inertial particles in homogeneous isotropic turbulence," *Journal of Computational Physics*, vol. 242, pp. 809–827, 2013.